



APPROVED FOR PUBLIC RELEASE, DISTRIBUTION UNLIMITED

ALEX(02)-TR-75-01-PART B

86-0158

LEVEL

(1)

COUNTEREVASION STUDIES

SEMI-ANNUAL TECHNICAL REPORT NO. 4 - PART B

1 NOVEMBER 1974 TO 30 APRIL 1975

AD A101468

TEXAS INSTRUMENTS INCORPORATED  
Equipment Group  
Post Office Box 6015  
Dallas, Texas 75222

Contract No. F44620-73-C-0055  
Amount of Contract: \$294,749  
Beginning 23 April 1973  
Ending 30 June 1975

Prepared for  
AIR FORCE OFFICE OF SCIENTIFIC RESEARCH

Sponsored by

ADVANCED RESEARCH PROJECTS AGENCY  
Nuclear Monitoring Research Office  
ARPA Program Code No. F10  
ARPA Order No. 1827

DTIC  
S E N T I M E N T  
JUL 1 71981  
H

30 May 1975

DTIC FILE COPY

Acknowledgment: This research was supported by the Advanced Research Projects Agency, Nuclear Monitoring Research Office, under Project VELA-UNIFORM, and accomplished under the direction of the Air Force Office of Scientific Research under Contract F44620-73-C-0055.

817 13007

Equipment Group



APPROVED FOR PUBLIC RELEASE, DISTRIBUTION UNLIMITED

(14) T I - ALEX(02)-TR-75-0: PART 2

- PT-B

(6) COUNTEREVASION STUDIES

(9) SEMI-ANNUAL TECHNICAL REPORT NO. 4 (PART B),  
1 NOVEMBER 1974 TO 30 APRIL 1975

Prepared by  
10 Stephen S. Lane and David Sun

TEXAS INSTRUMENTS INCORPORATED

Equipment Group  
Post Office Box 6015  
Dallas, Texas 75222

(12) 43

(13) Contract No. F44620-73-C-0055

Amount of Contract: \$294,749

Beginning 23 April 1973  
Ending 30 June 1975

ARPA Order-  
1827

Prepared for  
AIR FORCE OFFICE OF SCIENTIFIC RESEARCH

Sponsored by

ADVANCED RESEARCH PROJECTS AGENCY

Nuclear Monitoring Research Office

ARPA Program Code No. F10

ARPA Order No. 1827

Acquisition Ref.	X
Project Ref.	
Program Ref.	
Contract Ref.	
By	
Distribution/	
Availability Codes	
Avail and/or	
Dist	Special
A	

(11) 30 May 1975

Acknowledgment: This research was supported by the Advanced Research Projects Agency, Nuclear Monitoring Research Office, under Project VELA-UNIFORM, and accomplished under the direction of the Air Force Office of Scientific Research under Contract F44620-73-C-0055.

405076  
Equipment Group *SLT*

## UNCLASSIFIED

SECURITY CLASSIFICATION OF THIS PAGE (When Data Entered)

REPORT DOCUMENTATION PAGE		READ INSTRUCTIONS BEFORE COMPLETING FORM
1. REPORT NUMBER	2. GOVT ACCESSION NO.	3. RECIPIENT'S CATALOG NUMBER
		AD-A202 468
4. TITLE (and Subtitle)	5. TYPE OF REPORT & PERIOD COVERED	
COUNTEREVASION STUDIES	Semi-Annual Technical	
7. AUTHOR(s)	6. PERFORMING ORG. REPORT NUMBER	
Stephen S. Lane and David Sun	ALEX(02)-TR-75-01-PART B	
9. PERFORMING ORGANIZATION NAME AND ADDRESS	8. CONTRACT OR GRANT NUMBER(s)	
Texas Instruments Incorporated Equipment Group Dallas, Texas 75222	T44620-73-C-0055 ✓	
11. CONTROLLING OFFICE NAME AND ADDRESS	10. PROGRAM ELEMENT, PROJECT, TASK AREA & WORK UNIT NUMBERS	
Advanced Research Projects Agency Nuclear Monitoring Research Office Arlington, Virginia 22209	ARPA Program Code No. F10	
14. MONITORING AGENCY NAME & ADDRESS (if different from Controlling Office)	12. REPORT DATE	
Air Force Office of Scientific Research 1400 Wilson Boulevard Arlington, Virginia 22209	30 May 1975	
16. DISTRIBUTION STATEMENT (of this Report)	13. NUMBER OF PAGES	
	40	
17. DISTRIBUTION STATEMENT (of the abstract entered in Block 20, if different from Report)	15. SECURITY CLASS. (of this report)	
	UNCLASSIFIED	
18. SUPPLEMENTARY NOTES	16a. DECLASSIFICATION DOWNGRADING SCHEDULE	
ARPA Order No. 1827		
19. KEY WORDS (Continue on reverse side if necessary and identify by block number)		
Seismology Complex cepstrum Peaceful nuclear explosions Multiple nuclear explosions		
20. ABSTRACT (Continue on reverse side if necessary and identify by block number)		
It is shown that the complex cepstrum technique is most effective when simple signals are removed from the observed waveform in the order of their arrival. Cepstrum analysis of teleseismic short-period P-waves from fifteen presumed peaceful nuclear explosions in Eurasia suggests that nine contained more than one direct phase. This may indicate the possible multiple explosions or may well be just due to the surface		

**UNCLASSIFIED**

SECURITY CLASSIFICATION OF THIS PAGE(When Data Entered)

20. Continued

reverberations. Five of these events contained presumed depth phases of amplitude roughly twice that of the direct phase. It is conjectured that some form of surface focusing the up-going energy or restricted propagation of the direct phase might be responsible for this fact. Delay time as found by the cepstrum analysis of the same event at two stations are in satisfactory agreement, although the corresponding amplitude differs somewhat.

**UNCLASSIFIED**

SECURITY CLASSIFICATION OF THIS PAGE(When Data Entered)

## ABSTRACT

It is shown that the complex cepstrum technique is most effective when simple signals are removed from the observed waveform in the order of their arrival. Cepstrum analysis of teleseismic short-period P-waves from fifteen presumed peaceful nuclear explosions in Eurasia suggests that nine contained more than one direct phase. This may indicate the possible multiple explosions or may well be just due to the surface reverberations. Five of these events contained presumed depth phases of amplitude roughly twice that of the direct phase. It is conjectured that some form of surface focusing the up-going energy or restricted propagation of the direct phase might be responsible for this fact. Delay time as found by the cepstrum analysis of the same event at two stations are in satisfactory agreement, although the corresponding amplitude differs somewhat.

## TABLE OF CONTENTS

SECTION	TITLE	PAGE
	ABSTRACT	iii
I.	INTRODUCTION	I-1
II.	CEPSTRAL FILTERING SEQUENCE	II-1
III.	EXPERIMENTAL RESULTS	III-1
IV.	CONCLUSIONS	IV-1
V.	REFERENCES	V-1
	APPENDIX A - WAVEFORMS FROM THE CEPSTRUM ANALYSIS	A-1

## LIST OF FIGURES

FIGURE	TITLE	PAGE
III-1	LOCATIONS OF PRESUMED UNDERGROUND NUCLEAR EXPLOSIONS	III-2
III-2	CORRELATION COEFFICIENT VERSUS AMPLITUDE RATIO	III-6
III-3	P-pP DELAY TIME AND EVENT DEPTH VERSUS MAGNITUDE	III-10
A-1	PNE/710/71	A-3
A-2	PNE/1022/71	A-4
A-3	PNE/1222/71	A-5
A-4	PNE/709/72	A-6
A-5	PNE/820/72	A-8
A-6	PNE/921/72	A-9
A-7	PNE/1003/72	A-10
A-8	PNE/1124/72-2	A-12
A-9	PNE/815/73	A-14
A-10	PNE/828/73	A-15
A-11	PNE/919/73	A-16

## LIST OF TABLES

TABLE	TITLE	PAGE
III-1	PRESUMED PEACEFUL UNDERGROUND NUCLEAR EXPLOSIONS IN EURASIA	III-3
III-2	CEPSTRUM DECOMPOSITIONS OF PRESUMED PEACEFUL UNDERGROUND NUCLEAR EXPLOSIONS IN EURASIA	III-4
III-3	CEPSTRUM ANALYSIS RESULTS OF SEVEN EVENTS RECORDED AT DIFFERENT STATIONS	III-7

## SECTION I INTRODUCTION

In previous reports (Lane, 1973; Lane and Sun, 1974a; Lane and Sun, 1974b), the applicability of the complex cepstrum technique to the problem of separating naturally and synthetically mixed seismic signals into simple waveforms has been considered for various cases. Of particular interest in counterevasion studies is the separation of the signal from a single underground nuclear explosion into direct and surface-reflected phases, and these studies showed that with adequate signal-to-noise ratio this is possible for signal time separations down to 0.1 seconds, although for normally buried explosions low signal-to-noise ratio, limits time resolution to about 0.4 seconds. The theoretical basis for the cepstrum's performance was also presented in these papers.

The present work is concerned with another problem in counterevasion, that of the resolution of multiple underground nuclear explosions into their constituent parts. A theoretical discussion of the order in which this should be done is presented, followed by the results of the cepstral analysis of a number of seismic events presumed to be peaceful underground nuclear explosions (PNE's) in Eurasia.

## SECTION II

### CEPSTRAL FILTERING SEQUENCE

Here we consider the problem of deconvolving a waveform consisting of more than two simple signals. In such a case there are a number of sequences in which the cepstrum can be filtered. It will be shown that only two such sequences are useful in practice.

Consider the case of three signals which are identical except for their scale factors, taken to be 1,  $a_1$  and  $a_2$ . The first signal is represented by  $s(n)$ , and the signals arrive at times 0,  $n_1$ , and  $n_2$ , where the  $n_i$ 's are in units of the sampling time. Thus the mixed signal  $x(n)$  is

$$x(n) = s(n) + a_1 s(n-n_1) + a_2 s(n-n_2) . \quad (\text{II-1})$$

Then an extension of the development by Lane and Sun (1974b) shows that the complex cepstrum of the mixed signal is

$$\hat{x}(n) = \hat{s}(n) + \sum_{k=1}^{\infty} \sum_{r=0}^k (-1)^{k+r} \frac{(k-r)!}{r!(k-r)!} a_1^{k-r} a_2^r \delta\{n - kn_1 + r(n_1 - n_2)\} \quad (\text{II-2})$$

where  $\hat{s}(n)$  is the cepstrum of  $s(n)$ , the double sum represents the contribution of the multipath operator, and the delta function has its usual meaning.

Points where the argument of the delta function is zero are cepstral peaks.

Ideally the effect of any of the later arrivals can be removed by zeroing the appropriate cepstral peaks. In practice, however, this cannot be done, for the following reasons. First, the precise locations of the cepstral

peaks are unknown before filtering. Next, real data peaks are not isolated points but have some width and may therefore interfere with one another. Finally, for some combination of delay times even sharp peaks will lie atop one another. This will always happen when, for example,  $n_2 = 2n_1$ . Thus it is impossible to remove the peaks due to one later signal without disturbing those due to the others, even if accurate knowledge of the  $n_i$  is available.

In this situation the correct procedure is to zero every cepstral peak, retaining only  $\hat{s}(n)$ . This is done with the short-pass filter, which sets every cepstral point beyond some time to zero without disturbing those at shorter times. These earlier points will be due to  $\hat{s}(n)$  alone if the filter point falls before the time of the first multipath arrival. From  $\hat{s}(n)$  the original signal  $s(n)$  in the sequence can be recovered, and subtraction of  $s(n)$  from  $x(n)$  yields the remaining waveforms. Short-pass filtering can then be used to extract the first signal of this new sequence in the same manner as above. This procedure can be repeated a number of times but is ultimately limited to about six arrivals by small but cumulative inaccuracies in the estimation procedure.

There is a case where a different filtering sequence is necessary, however. The  $n$ -th point of the input trace must be multiplied by an exponential weighting factor  $\alpha^n$ , where  $\alpha < 1.0$ , in order that the multipath operator be minimum phase and thus completely represented in the cepstrum. The signals recovered by filtering are then unweighted by multiplying by  $\alpha^{-n}$ . If the trace is long and  $\alpha$  is small, large oscillations will appear in the unweighted outputs towards their ends due to the multiplication of noise by large values of the factor  $\alpha^{-n}$ . These oscillations completely obscure the motion of interest, and can only be eliminated by increasing the weighting factor  $\alpha$ , at the expense of making the multipath operator mixed phase. Useful results can still be obtained in the mixed phase case by filtering later in the cepstrum, because later arrivals may be represented completely at large values of  $\alpha$ .

where early ones are not. Some distortion will be introduced by zeroing later cepstral peaks due to the second arrival, so this sequence is to be avoided whenever possible.

### SECTION III EXPERIMENTAL RESULTS

Here we present the results of cepstral analysis of a number of presumed underground nuclear explosions away from normal test sites in Eurasia, assumed to be for some peaceful use. All such events occurring through 1973 for which good array data were available were examined. Nordyke (1974) presents information for these events as well as for others for which waveforms were not available. It is hoped that these analyses will prove useful to others investigating these events, and that the results themselves will help to establish the validity of the method.

Fifteen events were recorded with good signal-to-noise ratio at LASA during this time. Three of them were far enough from NORSAR to produce useable teleseismic records there, and two were recorded at Mould Bay, Canada. Table III-1 presents source information for these events, and establishes a system of nomenclature for them. Event locations are shown in Figure III-1.

For each event, the waveform recorded at LASA was separated into its constituent parts, which were identified as being either direct p phases or as surface reflections on the basis of the sign of their first motion. The correlation coefficient between the first direct and depth phases was calculated wherever these phases were observed, except for PNE/902/69 and PNE/908/69, for which all analysis was conducted during a previous contract period. The results are presented in Table III-2, where all arrival times and amplitudes of later phases are measured relative to the first-arriving phase. The symbol  $s_i(n-n_i)$  stands for a direct phase delayed by  $n_i$  sample points of 0.1 second duration each. Depth phases are represented by  $s'_i(n-n_i)$ . Complicated

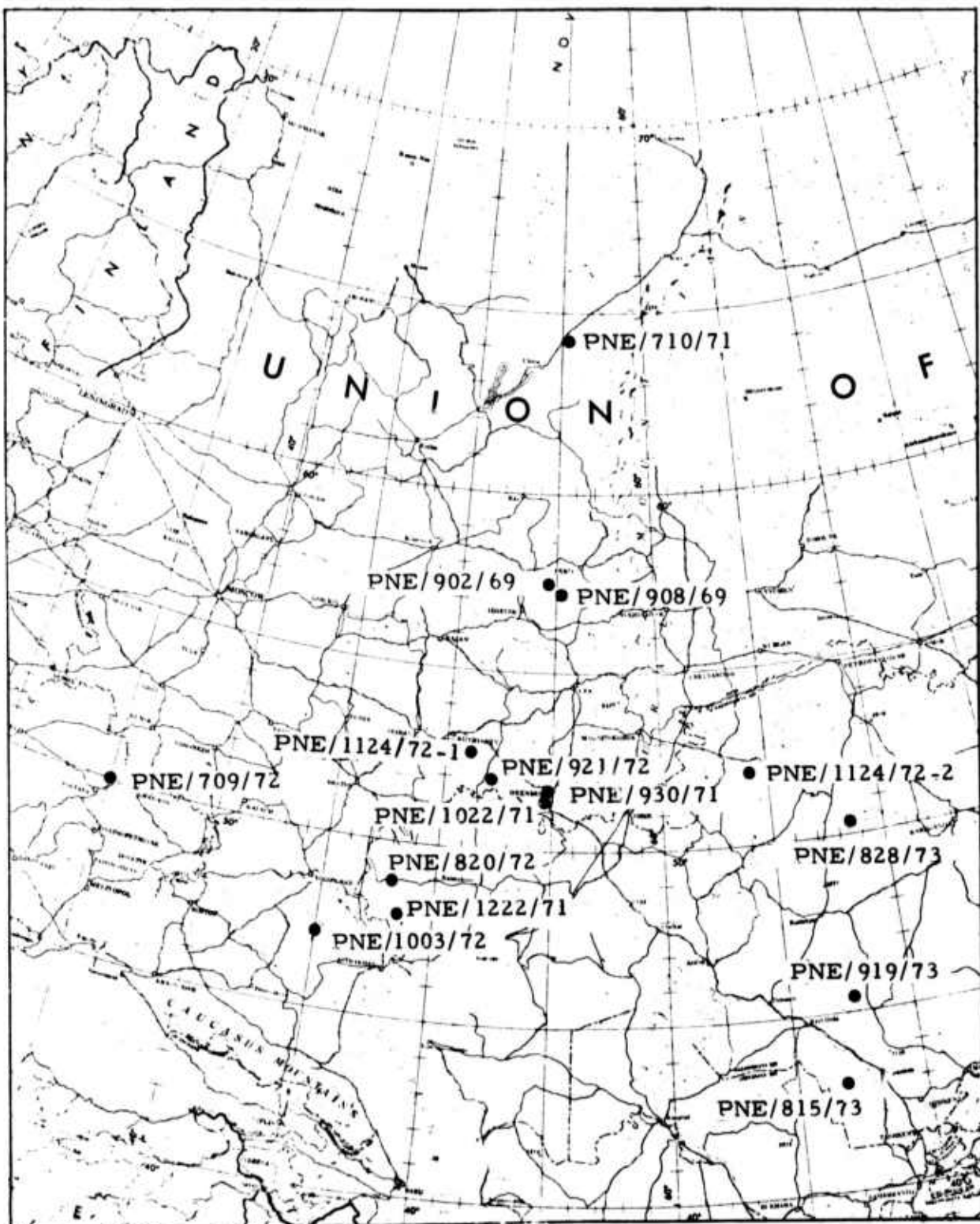


FIGURE III-1  
LOCATIONS OF PRESUMED UNDERGROUND  
NUCLEAR EXPLOSIONS

TABLE III-1  
PRESUMED PEACEFUL UNDERGROUND NUCLEAR  
EXPLOSIONS IN EURASIA

Event Identification	Date	Location		$\Delta^\circ$ To LASA	$\Delta^\circ$ To NORSSAR	$m_b$
		Lat $^\circ$ N	Lon $^\circ$ E			
PNE/902/69	69-09-02	57.420	54.850	74.70	22.43	4.9
PNE/908/69	69-09-08	57.370	55.110	75.11	24.00	4.9
PNE/710/71	71-07-10	64.168	55.183	68.17	20.34	5.3
PNE/1022/71	71-10-22	51.575	54.536	80.34	25.45	5.3
PNE/1222/71	71-12-22	47.872	48.222	82.83	24.87	6.0
PNE/709/72	72-07-09	49.900	35.200	77.79	17.47	5.0
PNE/820/72	72-08-20	49.462	48.179	81.31	23.74	5.7
PNE/921/72	72-09-21	52.127	51.994	79.42	23.87	5.1
PNE/1003/72	72-10-03	46.848	45.010	83.11	24.11	5.8
PNE/1124/72-1	72-11-24	52.779	51.067	78.64	23.03	4.7
PNE/1124/72-2	72-11-24	51.843	64.152	81.11	29.97	5.2
PNE/815/73	73-08-15	42.711	67.410	90.41	37.87	5.3
PNE/828/73	73-08-28	50.550	68.395	82.64	32.84	5.3
PNE/919/73	73-09-19	45.635	67.850	87.51	35.94	5.2
PNE/930/73	73-09-30	51.608	54.582	80.31	25.45	5.2

TABLE III-2

CEPSTRUM DECOMPOSITIONS OF PRESUMED PEACEFUL UNDERGROUND  
NUCLEAR EXPLOSIONS IN EURASIA

Event Identification	Cepstrum Analysis Results	Amplitude Ratio	$P^P$ Correlation Coefficient
PNE/902/69	$x(n) = s_1(n) + s'_1(n-6) + s_2(n-9) + s'_2(n-14) + s_3(n-20)$	1 : 1 : 0.75 : 0.75 : 0.47	—
PNE/908/69	$x(n) = s_1(n) + s'_1(n-6) + s_2(n-9) + s'_2(n-14) + s_3(n-20)$	1 : 1 : 0.75 : 0.75 : 0.47	—
PNE/710/71	$x(n) = s_1(n) + s'_1(n-5) + x_2(n-9)$	1 : 1.5	0.888
PNE/1022/71	$x(n) = s_1(n) + s'_1(n-6)$	1 : 2.25	0.857
PNE/1222/71	$x(n) = s_1(n) + s'_1(n-7)$	1 : 1.15	0.910
PNE/709/72	$x(n) = s_1(n) + s'_1(n-5) + s_2(n-10) + s'_2(n-16)$	1 : 1.05 : 0.57 : 0.57	0.873
PNE/820/72	$x(n) = s_1(n) + s'_1(n-7) + s_2(n-12)$	1 : 2.42 : 2.25	0.925
PNE/921/72	$x(n) = s_1(n) + s'_1(n-5) + s_2(n-20)$	1 : 1.90 : 1.58	0.731
PNE/1003/72	$x(n) = s_1(n) + s'_1(n-6) + s_2(n-12) + s'_2(n-18) + s_3(n-25)$	1 : 1.85 : 1.44 : 1.92 : 2.0	0.957
PNE/1124/72-2	$x(n) = s_1(n) + s'_1(n-5) + s_2(n-10) + s'_2(n-15) + s_3(n-20)$	1 : 1.05 : 1.24 : 0.91 : 1.40	0.910
PNE/1124/72-1	$x(n) = s_1(n)$	—	—
PNE/815/73	$x(n) = s_1(n) + s'_1(n-6)$	1 : 1.95	0.759
PNE/828/73	$x(n) = s_1(n) + s_2(n-9)$	1 : 0.67	—
PNE/919/73	$x(n) = s_1(n) + s'_1(n-8) + s_2(n-13) + s'_2(n-18)$	1 : 1.04 : 0.38 : 0.31	0.981
PNE/930/73	$x(n) = s_1(n)$	—	—

later arrivals which clearly consist of more than one phase but could not be resolved with precision up to our usual standards are represented by  $x_i(n-n_i)$  or by  $x'_i(n-n_i)$ , if the sign of their first motion was positive or negative, respectively. Waveforms of the original mixed signals,  $x(n)$ , and those of the cepstrum resolved signals,  $s_i(n)$ ,  $s'_i(n)$ ,  $x_i(n)$ , and  $x'_i(n)$  are given in Appendix A.

The most striking features of this table are the large amplitudes of some depth phases. The boundary conditions on stress at the free surface require that the ratio of the depth phase to direct phase amplitude be -1, and it must be numerically less if there is significant spalling or attenuation in the near surface layers. Thus amplitude ratios near 2.0, as observed here, are physically unreasonable on a simple model, and in fact have not been observed by us in presumed explosions from eastern Kazakh.

A weak decrease in correlation coefficient with increasing amplitude ratio is seen in the data as plotted in Figure III-2, but is probably not statistically significant. The average of the correlation coefficients for the presumed PNE's of amplitude ratio near 2.0 is 0.847, which compares well with the average correlation coefficient of 0.848 for 13 depth phases from eastern Kazakh presumed explosions. These measurements indicate that the decompositions with anomalously large amplitude ratio are nevertheless of good quality.

Table III-3 shows the results of cepstral analysis of the events which were available at more than one station, using the same notation as in Table III-2. Two Kazakh events are also included for comparison.

The first two presumed PNE's show excellent agreement between the results of analyses on LASA and Mould Bay data. This may be related to the fact that the event azimuth is almost the same at Mould Bay as at LASA. The other decompositions are also compatible with one another.

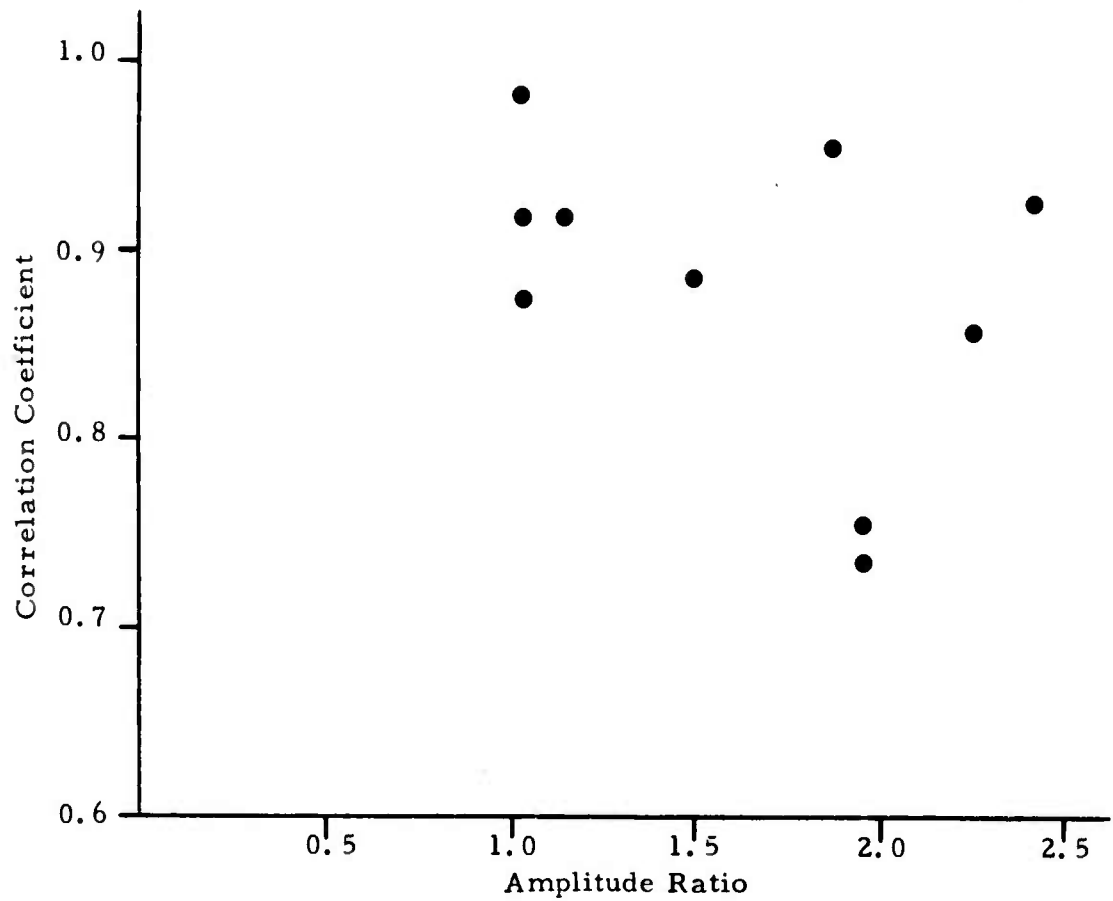


FIGURE III-2  
CORRELATION COEFFICIENT VERSUS AMPLITUDE RATIO

TABLE III-3  
CEPSTRUM ANALYSIS RESULTS OF SEVEN EVENTS RECORDED  
AT DIFFERENT STATIONS

Event Identification	Mould Bay Traces	Amplitude Ratio	LASA Traces	Amplitude Ratio
PNE/902/69	$x(n) = s_1(n) + s'_1(n-6) + s_2(n-9)$ $+ s'_2(n-14) + s_3(n-20)$	1 : 1.03 : 0.7 : 0.4	$x(n) = s_1(n) + s'_1(n-6) + s_2(n-9)$ $+ s'_2(n-14) + s_3(n-20)$	1 : 1 : 0.75 : 0.75 : 0.47
PNE/908/69	$x(n) = s_1(n) + s'_1(n-6) + s_2(n-9)$ $+ s'_2(n-14) + s_3(n-20)$	1 : 1.05 : 0.7 : 0.4	$x(n) = s_1(n) + s'_1(n-6) + s_2(n-9)$ $+ s'_2(n-14) + s_3(n-20)$	1 : 1 : 0.75 : 0.75 : 0.47
Event Identification	NORSAR Traces	Amplitude Ratio	LASA Traces	Amplitude Ratio
PNE/815/73	$x(n) = s_1(n) + s'_1(n-7)$	1 : 1.05	$x(n) = s_1(n) + s'_1(n-6)$	1 : 1.95
PNE/828/73	$x(n) = s_1(n) + x_2(n-9)$	1 : 0.35	$x(n) = s_1(n) + s_2(n-9)$	1 : 0.67
PNE/919/73	$x(n) = s_1(n) + x_1(n-6)$	1 : 0.5	$x(n) = s_1(n) + s'_1(n-8) + s_2(n-13)$ $+ s'_2(n-18)$	1 : 1.04 : 0.38 : 0.31
EKZ/294/04N	$x(n) = s_1(n) + s'_1(n-4) + s_2(n-8)$	1 : 1.3 : 1.6	$x(n) = s_1(n) + s'_1(n-5)$	1 : 0.93
KAZ/081/04N	$x(n) = s_1(n) + s'_1(n-6)$	1 : 0.74	$x(n) = s_1(n) + s'_1(n-7)$	1 : 1.0

Agreement for amplitudes and delay times is good for PNE/815/73. The second arrival in PNE/828/73 at NORSAR is a direct one, at the same time as the second direct phase at LASA and contains subsequent arrivals which could not be resolved due to their low level compared to the coda from the first event. PNE/919/73 as recorded at NORSAR also contains an unresolved later phase, whose first motion is clearly negative, and which might be composed of a depth phase plus a later direct arrival as in the LASA analysis.

Those PNE events for which depth phases were found have reasonable amplitude ratios at NORSAR, when observed there, of about half the value observed at LASA. It is also interesting that the second event claimed for PNE/828/73 has a different amplitude ratio at NORSAR than at LASA.

These results strengthen the belief that the arrivals presented in Table III-2 represent real seismic waves and are not the result of forcing the data to agree with a pre-assumed model. However, the amplitude estimates of these arrivals are quite variable.

Support for this view also comes from the Kazakh events. Here the observed delay times agree within a sample point, but the amplitude ratios disagree by about 30% even for the clear high signal-to-noise ratio events studied.

Since the direct and reflected phases follow the same seismic path except near the shot point, it is reasonable to look there for an explanation of the observed anomalies. There are two possibilities - either the direct phase is unusually small, or the surface phase is unusually large. The first would arise if some special conditions at the shot point inhibited the propagation of energy downward. This might be the case since presumably these explosions had some technological purpose. This same mechanism might also be directional, explaining the variation in amplitude of the second direct arrival of PNE/828/73 as well as the variations in depth phase amplitudes.

The second possibility might occur if special topography focused the surface-reflected energy somewhat. The mountainous region where these events occurred might provide such topography which might also focus energy differently in different directions. Both of these explanations are highly speculative, however, and the only conclusions drawn here are that depth phase to direct phase amplitude ratios are quite variable from event to event, and from recording site to recording site, while identification of phases and measurements of delay times are probably accurate.

Depth phase delay times are plotted against event  $m_b$  in Figure III-3 for the presumed PNE's studied here. There is a weak increase in delay time with magnitude, and the observed times are not in conflict with those predicted by the cube-root scaling law shown as a solid line. This semi-empirical rule requires that contained explosions be buried at a depth in feet of at least  $h = W^{1/3}/400$ , where  $W$  is the yield in kilotons of TNT. An estimate of the near-surface p-wave velocity  $v$  leads to a delay time of  $2h/v$ , and this velocity was chosen to be 3.2 km/sec here. There is no reason to suppose that these explosions were buried near the depth necessary for containment, so divergences of the data from the solid line have little significance, except to suggest that these were not cratering explosions. The possible exception is PNE/1222/71, which fell below the cube root scaling curve at  $m_b = 6.0$ .

Although the evidence presented here supports the assumption that these events were multiple explosions it might possibly be due to surface effects such as reverberations. It would therefore be very desirable to analyze them, or others, at as many stations as possible. Identical decompositions at three or more stations for the same events would be much stronger evidence of their nature, especially if wide azimuthal coverage was obtained.

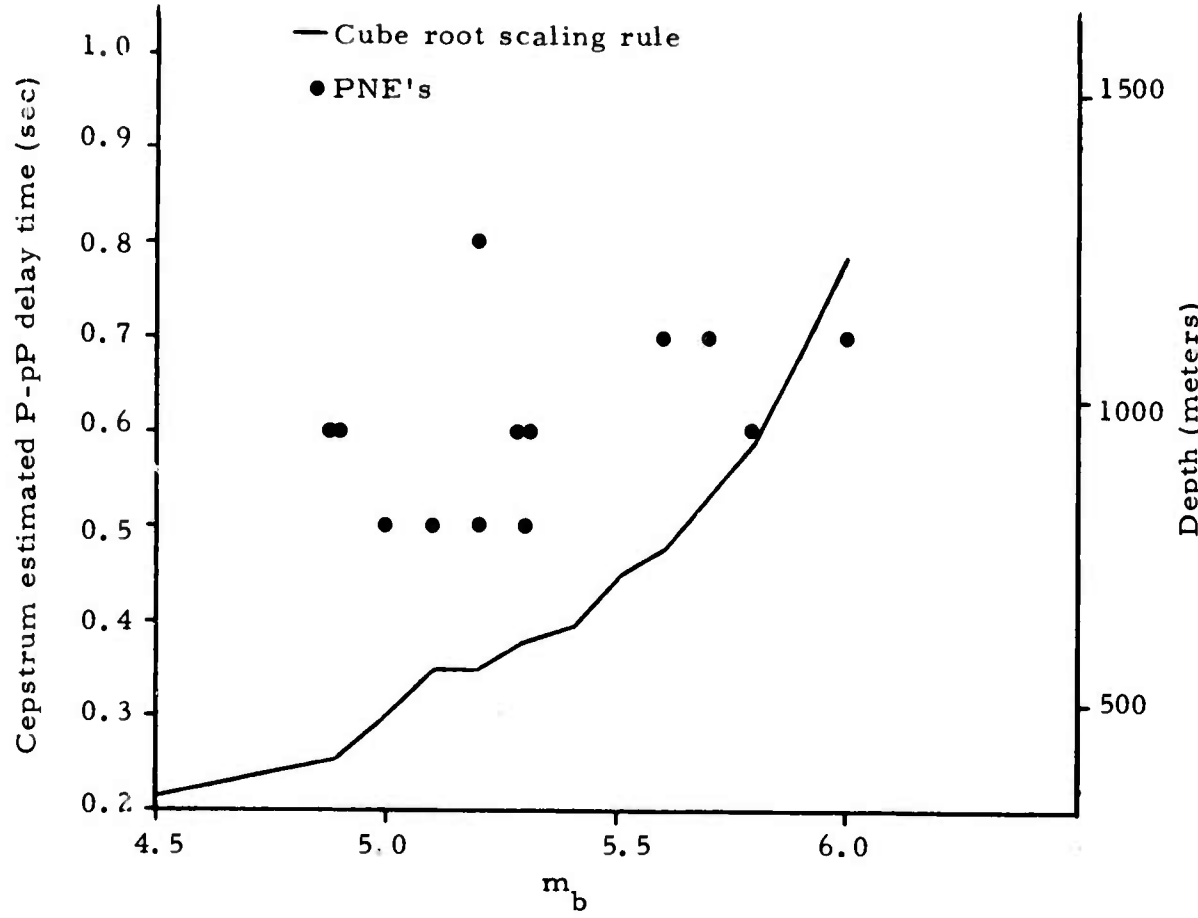


FIGURE III-3  
P-pP DELAY TIME AND EVENT DEPTH VERSUS MAGNITUDE

## SECTION IV CONCLUSIONS

Fifteen presumed peaceful nuclear explosions and two presumed Kazakh explosions have been processed here using the complex cepstrum technique developed previously by these authors. Depth phases were found for all but three of the PNE's, and could have been used as discriminants if required. Ten of the PNE's appear to be multiple explosions, with delay times up to 2.5 seconds in the case of one possible triple explosion.

The observed delay times of the depth phases are consistent with all of the events being contained. In this context it should be noted that the absence of a depth phase does not lead to the conclusion that a crater was formed, since the shock wave responsible for the depth phase arrives at the free surface while the latter is still intact. The crater is formed by the later expansion of the cavity gasses. Thus even a cratering event should produce a depth phase.

Correlation between observed direct and depth phases was high, and for the cases where the waveforms could be observed at two locations, agreement between times of depth phase arrival was good. However, anomalously high amplitudes were observed for the depth phase of some events at LASA, though not at NORSAR. Even for events with reasonable pP amplitudes at each array there was variation by a factor of two among the ratio between depth and direct phases. These results lead to the conclusions that:

- Cepstrum analysis can recover depth phases from real underground nuclear explosions in regions of complicated geology in a large majority of cases.

- Cepstrum analysis is believed to be able to resolve possible multiple arrivals in the real teleseismic short-period P-waves of a presumed explosion. However, the resolved multiple arrivals may come from a real multiple explosion or may be attributed to the effect of surface reverberations.
- Where the depth phase can be identified its delay time can be determined well within the accuracy required for discrimination.
- The cepstrum resolved depth phase amplitudes may be larger than the theoretically expected value by a factor of two. This may be caused by the surface focusing or directional propagation.

SECTION V  
REFERENCES

Lane, S. S., 1973, Semi-Annual Technical Report No. 1 - Part B, Texas Instruments Report Number ALEX(02)-TR-73-01-PART B, AFOSR Contract Number F44620-73-C-0055, Texas Instruments Incorporated, Dallas, Texas.

Lane, S. S., and D. Sun, 1974a, Semi-Annual Technical Report No. 2 - Part B, Texas Instruments Report Number ALEX(02)-TR-74-02-PART B, AFOSR Contract Number F44620-73-C-0055, Texas Instruments Incorporated, Dallas, Texas.

Lane, S. S., and D. Sun, 1974b, Semi-Annual Technical Report No. 3 - Part B, Texas Instruments Report Number ALEX(02)-TR-03-PART B, AFOSR Contract Number F44620-73-C-0055, Texas Instruments Incorporated, Dallas, Texas.

Nordyke, Milo D., 1973, A Review of Soviet Data on the Peaceful Uses of Nuclear Explosions, Report Number UCRL-51414, Lawrence Livermore Laboratory, University of California/Livermore.

## APPENDIX A

### WAVEFORMS FROM THE CEPSTRUM ANALYSIS

The waveforms of the original mixed signals and the cepstrum resolved signals, which are represented by  $x(n)$ ,  $s_i(n)$ ,  $s'_i(n)$ ,  $x_i(n)$  and  $x'_i(n)$  in Table III-2, are shown in the following figures. In these figures, the division along the time axis is 0.1 second. For each figure, the input signal to the cepstrum analysis is given first, and the cepstrum resolved waveforms follow. These output signals of the cepstrum analysis are given with the first arrivals shown as solid lines and the second arrivals shown as dashed lines. For the mixed signal which consists of only two single arrivals, such as the event PNE/1022/71 in Table III-2, the signal input to the cepstrum analysis is the original mixed signal  $x(n)$  and the output of the cepstrum analysis is the final decomposition shown in Table III-2. For the mixed signal which consists of more than two single arrivals, such as the event PNE/709/72 in Table III-2, the input to the cepstrum analysis can be either the original mixed signal  $x(n)$  or the reduced mixed signal  $x_i(n)$  (or  $x'_i(n)$ ). The final decomposition can be obtained by summing up all the intermediate outputs of the cepstrum analysis for the same event. As an example, consider event PNE/709/72. The intermediate outputs, shown in Figure A-4, are:

$$x(n) = s_1(n) + x'_1(n-5) \quad (A-1)$$

$$x'_1(n) = s_1(n) + x_2(n-5) \quad (A-2)$$

$$x_2(n) = s_2(n) + s'_2(n-6) . \quad (A-3)$$

The final decomposition is obtained by summing up equations (A-1) through (A-3), with appropriate time shifts in equations (A-2) and (A-3) as follows:

$$x(n) = s_1(n) + x'_1(n-5)$$

with

$$x'_1(n-5) = s'_1(n-5) + x_2(n-10)$$

and

$$x_2(n-10) = s_2(n-10) + s'_2(n-16).$$

Therefore,

$$x(n) = s_1(n) + s'_1(n-5) + s_2(n-10) + s'_2(n-16).$$

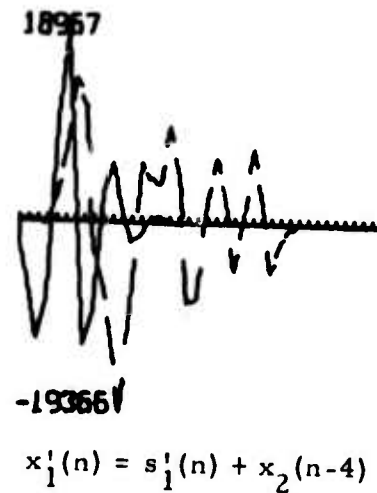
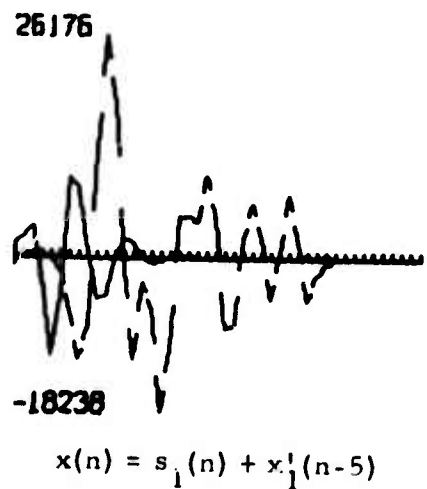
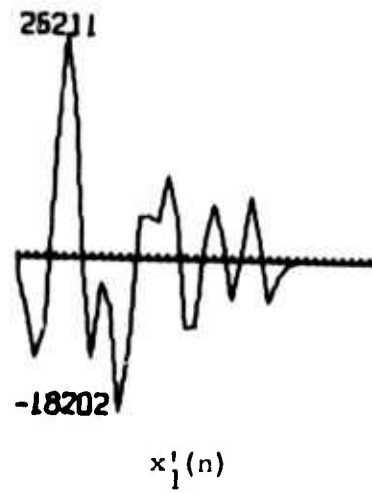
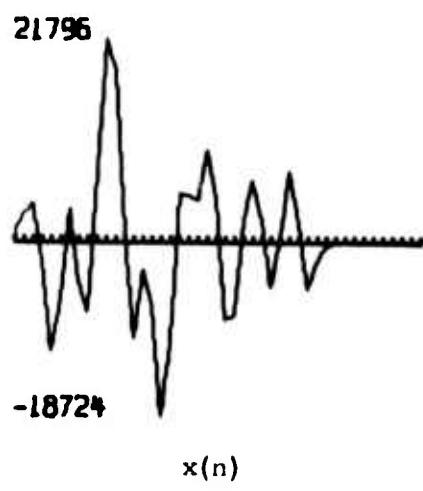
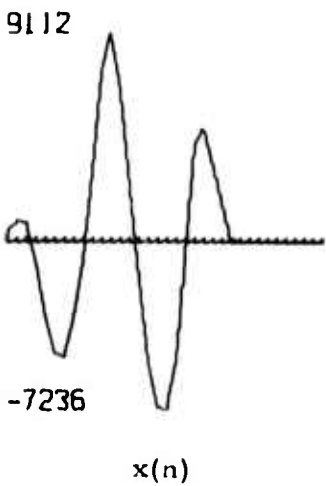


FIGURE A-1  
PNE/710/71



$$x(n) = s_1(n) + s'_1(n-6)$$

FIGURE A-2  
PNE/1022/71

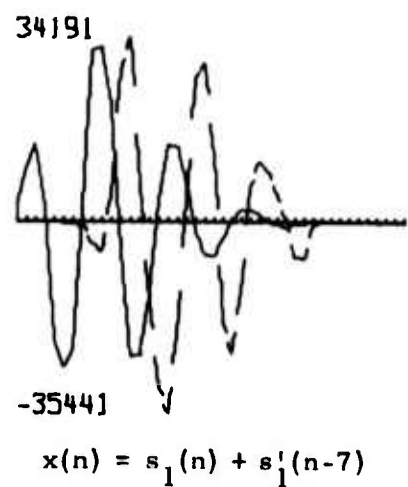
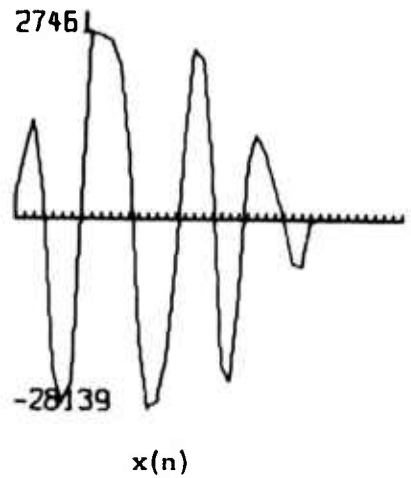
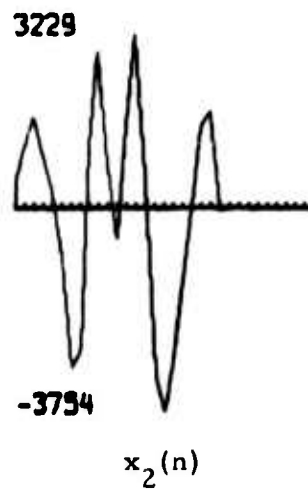


FIGURE A-3  
PNE/1222/71



FIGURE A-4a  
PNE/709/72



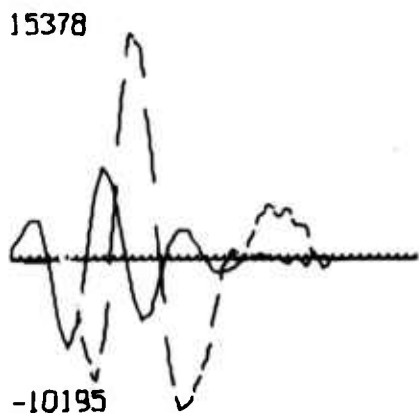
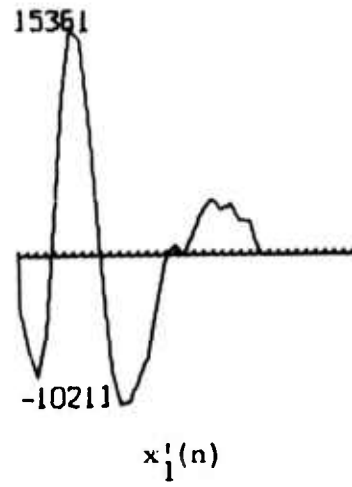
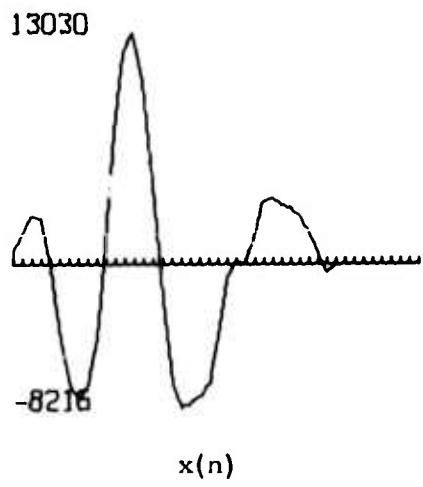
$$x_1'(n) = s_1'(n) + x_2(n-5)$$



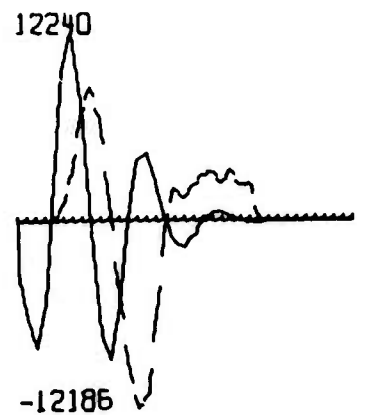
$$x_2(n) = s_2(n) + s_2'(n-6)$$

FIGURE A-4b

PNE/709/72

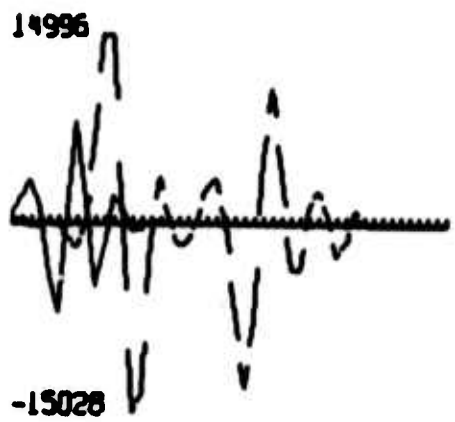
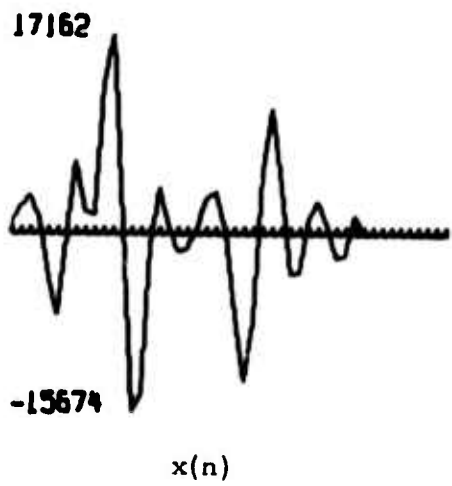


$$x(n) = s_1(n) + x_1'(n-7)$$

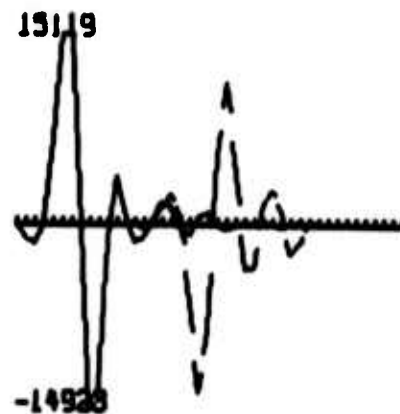


$$x_1'(n) = s_1'(n) + s_2(n-5)$$

FIGURE A-5  
PNE/820/72



$$x(n) = s_1(n) + x_1'(n-5)$$



$$x_1'(n) = s_1'(n) + s_2(n-15)$$

FIGURE A-6  
PNE/921/72

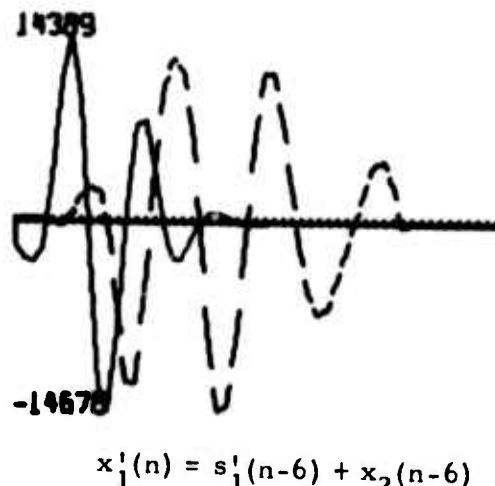
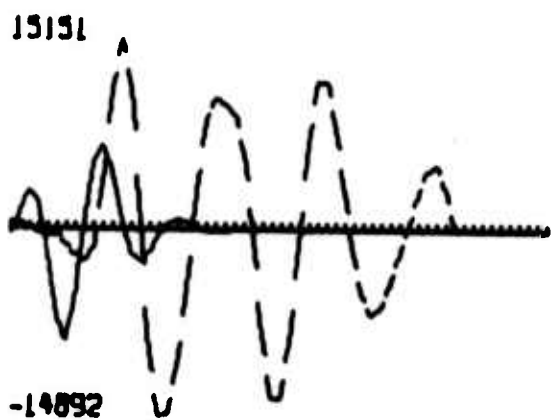
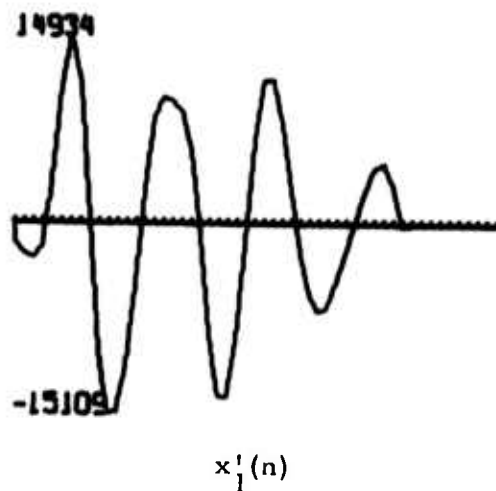
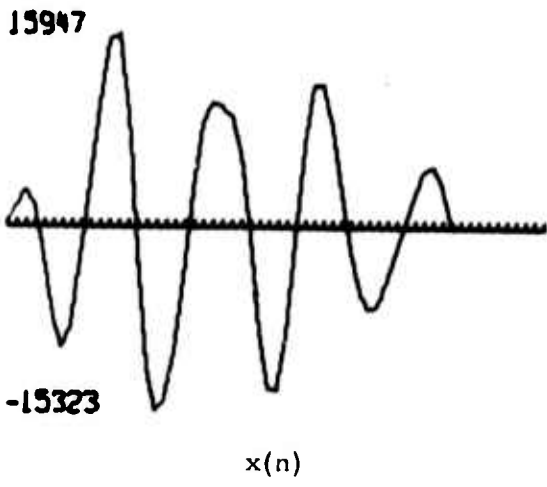


FIGURE A-7a  
PNE/1003/72

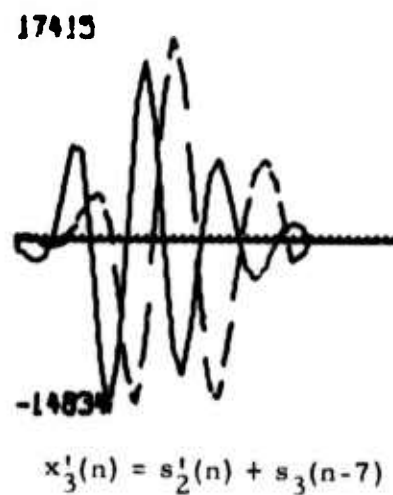
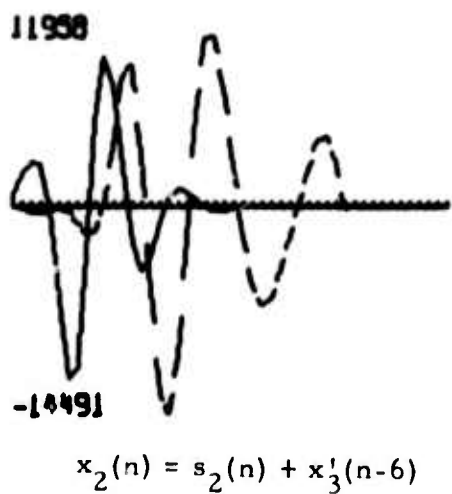
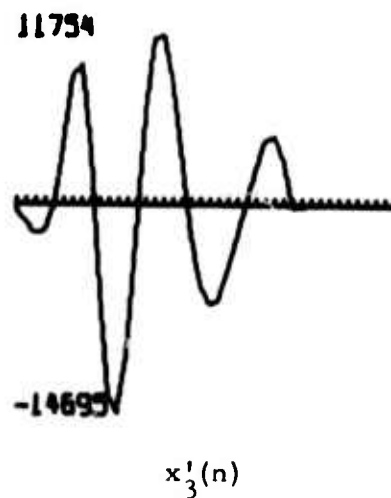
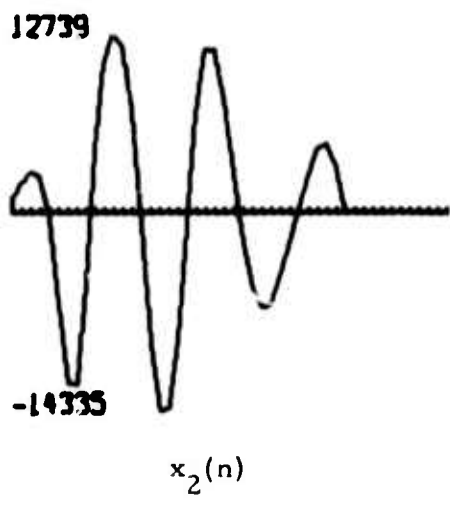


FIGURE A-7b  
PNE/1003/72

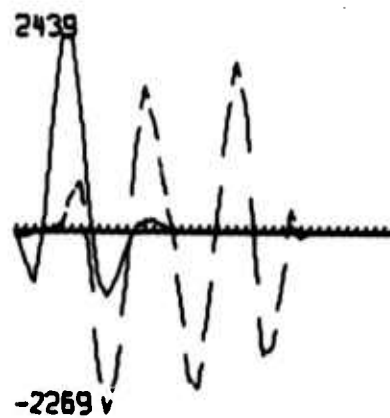
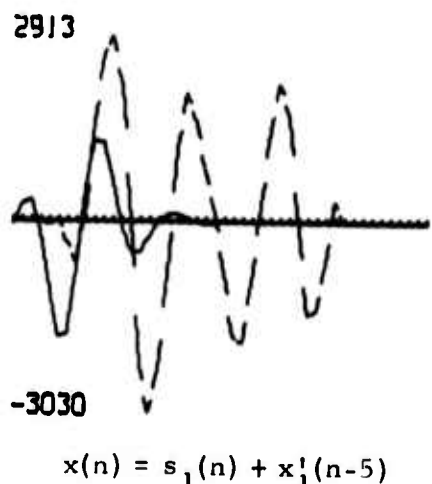
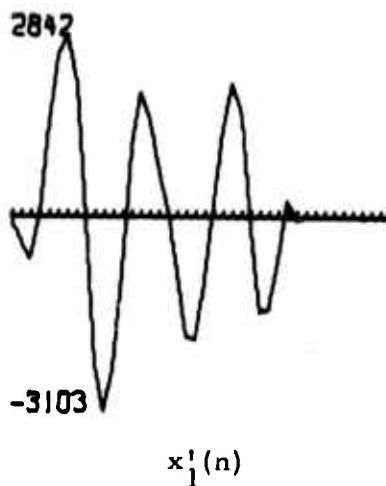
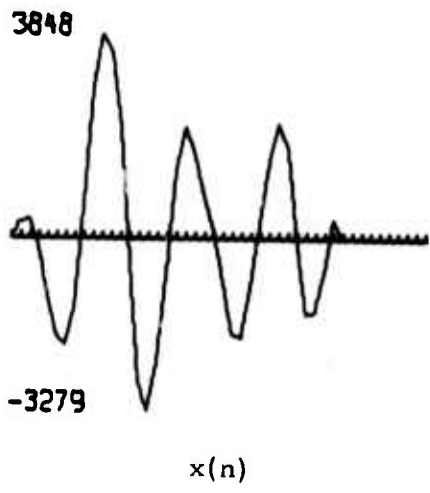


FIGURE A-8a  
PNE/1124/72-2

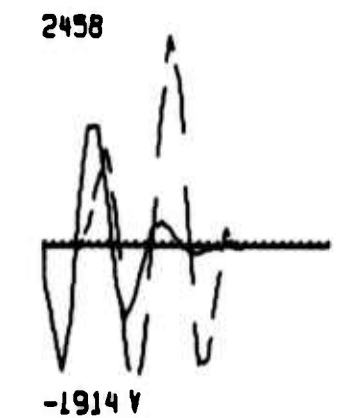
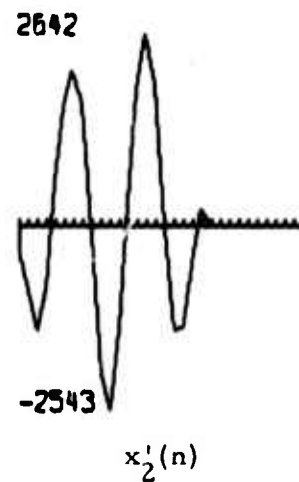
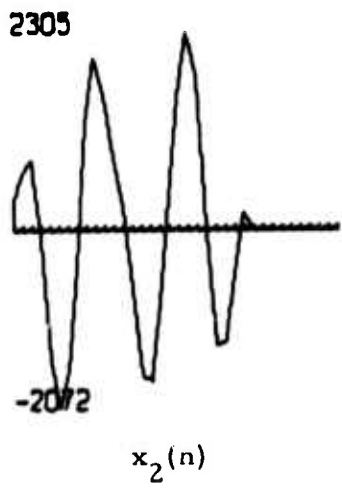


FIGURE A-8b  
PNE/1124/72-2

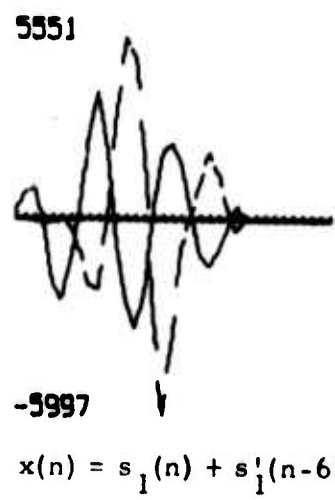
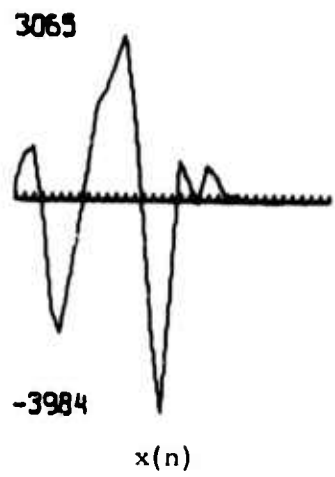
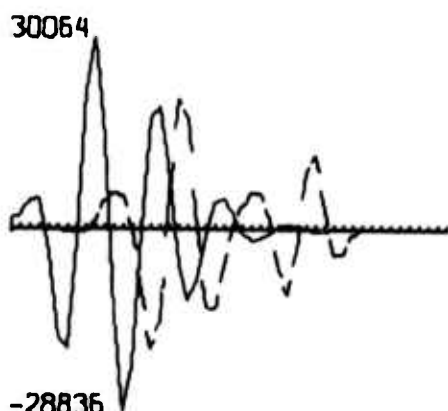
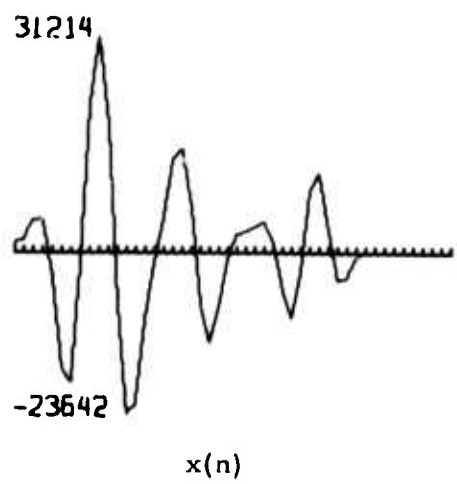


FIGURE A-9

PNE/815/73



$$x(n) = s_1(n) + s_2(n-9)$$

FIGURE A-10

PNE/828/73

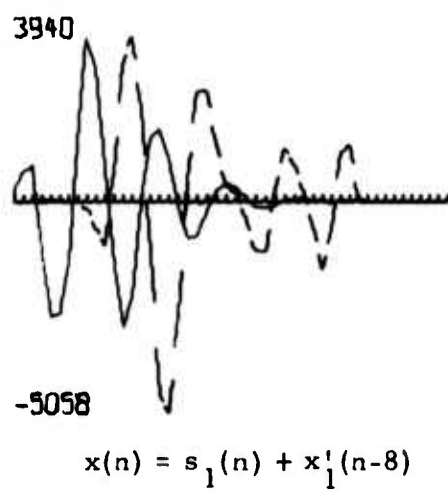
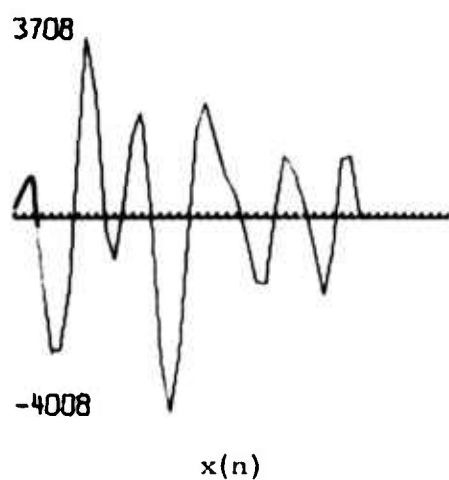
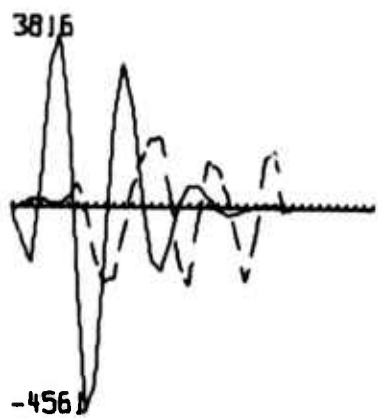
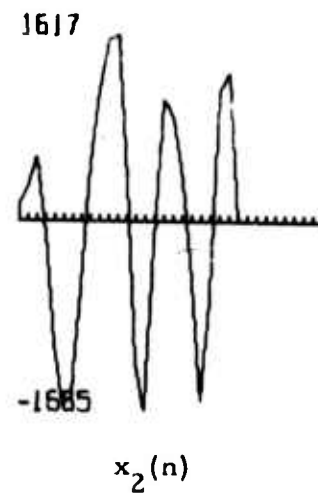
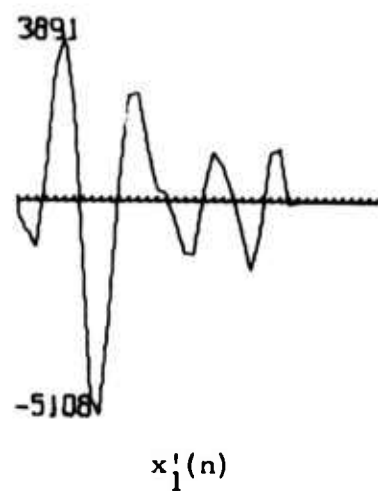


FIGURE A-11a

PNE/919/73



$$x_1'(n) = s_1'(n) + x_2(n-5)$$



$$x_2(n) = s_2(n) + s_2'(n-5)$$

FIGURE A-11b

PNE/919/73